PEM Electrolyzer with Nano-structured Electrodes for High Efficient Hydrogen Production

S. Rau, J. Colom Tomás, T. Smolinka, R.E. Fuentes, J.W. Weidner

PEM Electrolyzer with Nano-structured Electrodes for High Efficient Hydrogen Production

S. Rau, **J. Colom Tomás**, **T. Smolinka**, Fraunhofer Institute for Solar Energy Systems ISE, Heidenhofstrasse 2, 79110 Freiburg, Germany
R.E. Fuentes, **J.W. Weidner**, University of South Carolina, Center for Electrochemical Engineering, Columbia, SC 29208, USA

1   Introduction

Hydrogen as a secondary energy carrier can play an important role in our future energy economy. Hydrogen can be stored, transported in tanks or pipe lines, is clean burning, and can be directly and efficiently converted into electricity using fuel cells. However, the major barrier is how to generate and supply pure hydrogen directly. One of the most efficient and simple ways to obtain hydrogen with high purity is the proton exchange membrane (PEM) water electrolysis. The main advantages against alkaline and steam water electrolysis is the high efficiency, compact design and fast response time against fluctuating energy supply. Therefore coupling of renewable energies with PEM electrolyzers is more and more regarded because hydrogen from PEM water electrolysis can match energy demand with energy supply.

For using PEM water electrolysis only water and electricity is necessary to produce hydrogen as well as oxygen as a by-product. The core component of every PEM water electrolyzer is the electrode membrane assembly, the so-called MEA. The membrane is only conductive for protons and works furthermore as a gas separator to avoid gas mixing inside the cell. Unfortunately PEM water electrolyzers suffer from membrane degradation and high costs of membrane and catalyst production. Currently, one of the main challenges is the large overpotential at typical current densities at the anode, where oxygen evolution reaction (OER) occurs. The OER depends strongly on the chemical and structural properties of the surface, being mainly determined by the interactions between a metal or metal oxide on the surface. The metal or its oxide used should be stable and conductive. These catalysts are usually unsupported because of the high corrosive conditions at the anode. Based on heterogeneous catalysis, a support is chosen to enhance the catalyst and promote the desired reaction. In electrochemical systems carbon support is chosen because of its high conductivity, rather than enhancement of activity. Since the anode of the water electrolyzer is operated at potentials higher than 0.9 V, carbon can corrode [1]. This corrosion can create a loss of electrical contact necessary for the transport of electrons, thus decreasing the performance. Also, platinum can increase the rate of corrosion of carbon [2]. Due to these limitations, research activities are underway to find a support that can be stable at high potentials and can help with the kinetics of the oxygen evolution reaction.

Some supports used in heterogeneous catalysis are composed of metal oxides, not only because of activity towards the selected reaction, but also because they are inert and non-corrosive. Specifically, titanium dioxide has been investigated for catalytic applications and

has been proved that its anatase structure is a more active catalyst for oxidizing hydroxil compounds, than its other structures rutile and brookite. The problem with titanium dioxide, as it is with metal oxides, presents a barrier for the conduction of electrons at low temperatures. Morris *et al.* [3] studied mixtures of NbO_2 and TiO_2 sintered at high temperatures to form $Nb_{0.1}Ti_{0.9}O_2$, but the material becomes the more stable and less catalytically active rutile structure. Chen *et al.* [4] measured the conductivity of this material and found a conductivity of 0.2-1.2 S/cm and a surface area of 1.4 m^2/g. We have refined the synthesis method of $Nb_{0.1}Ti_{0.9}O_2$ (here referred to as $Nb-TiO_2$) [5] and used it to deposit nanoparticles for the OER.

2   Results and Discussion

To examine the crystal structure of the pure TiO_2 (obtained from Sigma-Aldrich) and $Nb-TiO_2$ (synthesized via the method by Fuentes *et al.* [5]) support materials, X-ray diffraction (XRD) was performed on a Rigaku 405S5. The XRD patterns were compared with reference spectra using the software JADE (Materials Data, Inc.). Figure 1 presents the XRD spectra for $Nb-TiO_2$. The vertical blue lines in the spectrum represent the XRD peaks for anatase Titania using JADE. The parameter for anatase matches every peak demonstrating a good anatase TiO_2 structure. No other crystalline phases were detected in the sample, including distinct niobium oxides structures. For the same synthesis in Cassiers *et al.* [6], the crystal phases obtained for TiO_2 were a mixture of anatase and rutile. For our synthesis method, it appears that the addition of niobium into the synthesis procedure helps to maintain and preserve the anatase structure.
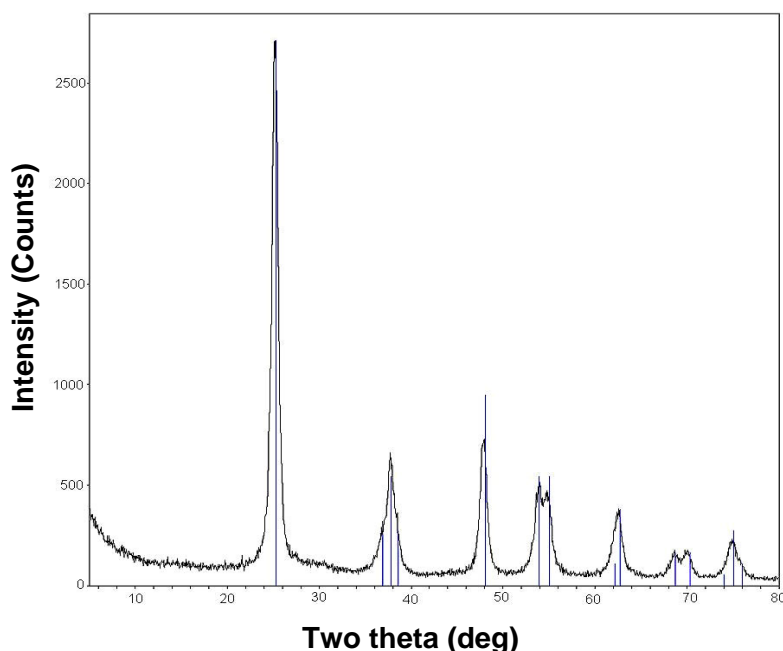

Figure 1:   X-Ray Diffraction data for Nb-TiO$_2$. The blue lines represent the guidelines for anatase TiO$_2$.

Furthermore Brunauer-Emmett-Teller (BET) surface areas measurements were performed using a Nova 2000 High speed gas adsorption analyzer. The surface areas were obtained using liquid nitrogen at 77 K and a 6 point BET was used for calculating the specific surface area. The adsorbate used for BET was nitrogen gas. For anatase Nb-TiO$_2$, the surface area was 197 m^2/g, which is only 16% lower than the surface area of carbon Vulcan XC-72R (usually the support of commercial catalysts for fuel cells). However, this surface area is sufficiently lower than the 613 m^2/g for pure TiO$_2$ reported by Cassiers *et al.* [6]. However, their material contained a mixture of anatase and rutile. The pure TiO$_2$ anatase obtained from Sigma-Aldrich had a surface area of 166 m^2/g. We also prepared a rutile form of Nb-TiO$_2$ by raising the anatase form to 1000°C for 5 hours. The resulting surface area decreased to 5.0 m^2/g. The pure TiO$_2$ rutile obtained from Sigma-Aldrich had a surface area of 273 m^2/g.

A series of electrical conductivity tests, shown in Figure 2, were performed using different platinum weight percent to determine how the quantity of a conductive metal affects the conductivity of the composite electrode (i.e., Pt plus Nb-TiO$_2$ support). Platinum metal was used in this measurement for convenience.
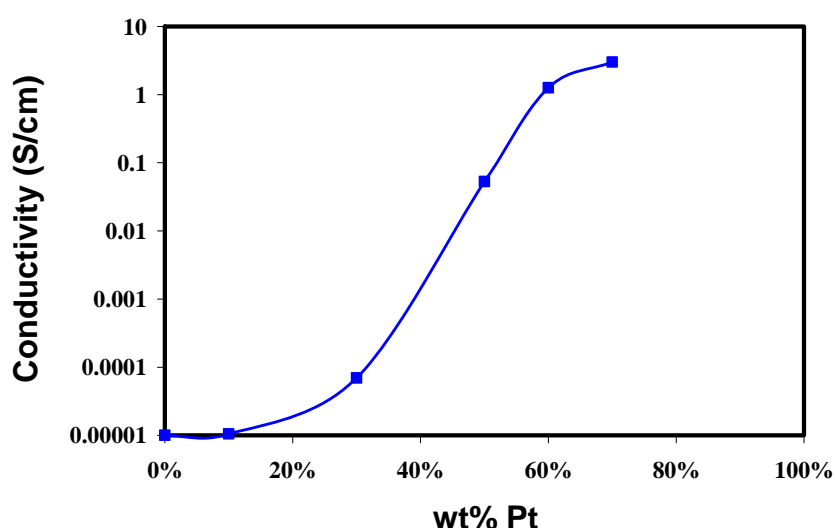

Figure 2:   **Conductivity of the composite electrode (i.e., Pt plus Nb-TiO$_2$ support) as a function of the weight percent loading of platinum.**

Increasing the Pt loading to 60% increased the conductivity of the composite electrode from 10^{-5} to 1.26 S/cm. These results indicate that the mixture of metal particles and oxide material creates a significantly less resistive path for the transportation of electrons.

To examine the particle-size distribution of bimetallic nanoparticles on the oxide supports, high resolution transmission electron microscopy (HRTEM) images were obtained and shown in Figure 3. These images are for 60 wt% PtRu on commercial anatase (A) and rutile (B) TiO$_2$. The bright rounded images are the bimetallic metals, platinum and ruthenium and the dark areas are the TiO$_2$. The anatase TiO$_2$ particles are round in shape with a particle size in diameter of 10 to 15 nm. The TiO$_2$ in its rutile form are presented in a more elliptical shape with higher particle size than anatase TiO$_2$. Generally at this high loading, the particles

are well dispersed in all the supports. Average particle size was determined and a histogram is also presented in Figure 3 next to HRTEM images. Around 100 particles were measured for each material and the average particle size determined for 60% PtRu/TiO$_2$ anatase (A) was 1.36 ± 0.29 nm and for 60% PtRu/TiO$_2$ rutile (B) was 1.77 ± 0.34 nm.
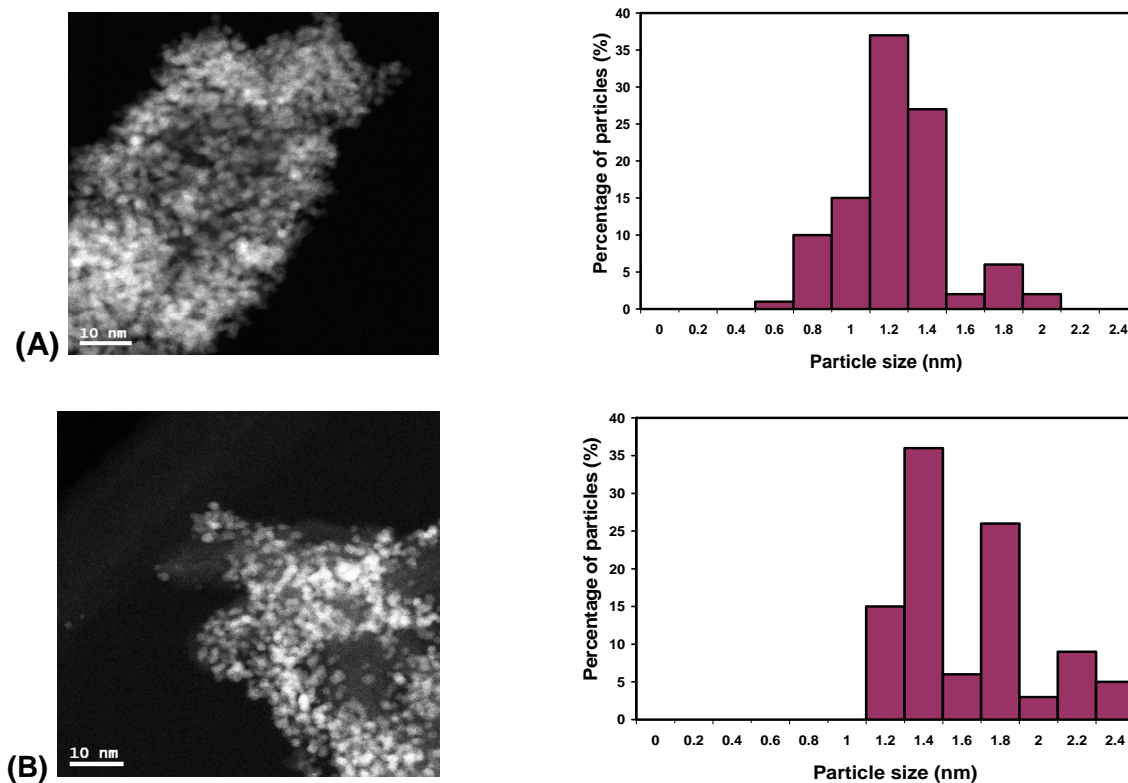

Figure 3: **HRTEM images and Histograms of (A) 60 wt% PtRu on anatase TiO$_2$ and (B) 60 wt% PtRu on rutile TiO$_2$.**

3   Benchmark Measurements

Performance and durability tests in PEM electrolyzers are necessary to compare these novel nano-structured materials with state-of-the-art MEAs. Therefore benchmark measurements from commercial MEAs are performed under different conditions like temperature and pressure variations. Benchmark measurements were performed in a 25 cm² single test cell. The test cell was delivered with deionized water on the anode and cathode side using a circulation pump. Under atmospheric pressure different temperature dependent curves are shown in Figure 4 in a galvanostatic mode. A titanium sinter plate with 75-100 µm spheric powder size as a current collector was used. The best cell performance was achieved by operating temperature of 343 K due to the faster kinetics of the reactions. Here 1.83 V can be obtained by current density of 1 A/cm^2. Marshall *et al.* [7] reported that voltage of 1.57 V at 1 A/cm^2 and 353 K are possible with Ir$_{0.6}$Ru$_{0.4}$O$_2$ anode and a 20 wt% Pt/C cathode. Figure 5 presents benchmark measurements for different operating pressures up to 50 bar by 343 K. It is clearly shown that higher pressures lead to higher voltage values, whereas the

difference with 15 mV by 1 A/cm^2 between 1 bar and 10 bar is rather small. The highest voltage with 2.11 V at 1 A/cm^2 is measured at a pressure of 50 bar, which yields in 14.1% higher cell performance comparable to atmospheric pressure.
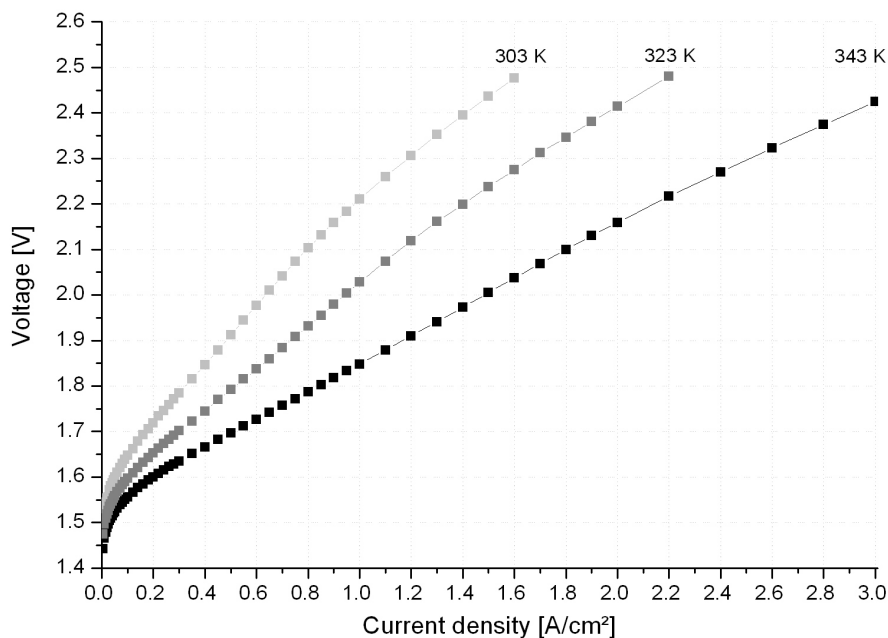

Figure 4: **Polarization curve of a 200 μm benchmark CCM Fumea$^®$ from FuMA-Tech using different operating temperatures and 0.1 MPa.**
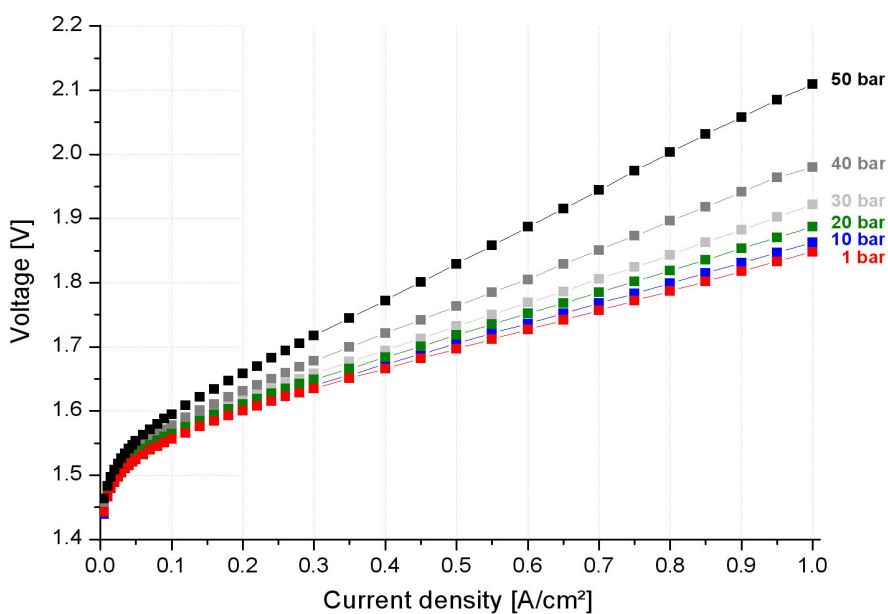

Figure 5: **Polarization curve of a 200 μm benchmark CCM Fumea$^®$ from FuMA-Tech using different operating pressures and 343 K.**

4   Conclusion

A Nb-TiO$_2$ support was synthesized with anatase and rutile crystalline structures. Since the Nb and Ti have similar ionic radius it is suggested that Nb is incorporated into the lattice. A surface-area analysis for the synthesized anatase Nb-TiO$_2$ gave 197 m^2/g, which is only 16% lower than carbon Vulcan XC-72R. The surface area was 19% higher than commercial anatase TiO$_2$. The surface area of the synthesize rutile Nb-TiO$_2$ was only 5.0 m^2/g. Particles with 60 wt% PtRu on anatase TiO$_2$ are round in shape, whereas 60 wt% PtRu on rutile TiO$_2$ have a more elliptical shape with higher particle size. For benchmarking, a high pressure 25 cm² electrolysis cell was constructed. First cell performance using commercial MEA showed a voltage of 1.83 V at 1 A/cm² and 343 K. With the same current density a voltage of 2.11 V was obtained by operating pressure of 50 bar. Further work is necessary to compare the new developed materials in a PEM electrolysis cell with benchmark measurements.

Acknowledgement

References

[1]   Young, A. P., Stumper, J., and Gyenge, E. (2009) Characterizing the Structural Degradation in a PEMFC Cathode Catalyst Layer: Carbon Corrosion. Journal of The Electrochemical Society, 156 (8), B913–B922.

[2]   Roen, L. M., Paik, C. H., and Jarvi, T. D. (2004) Electrocatalytic Corrosion of Carbon Support in PEMFC Cathodes. Electrochemical and Solid-State Letters, 7 (1), A19–A22.

[3]   Morris, D., Dou, Y., Rebane, J., Mitchell, C. E. J., Egdell, R. G., D., Law, S. L., Vittadini, A., and Casarin, M. (2000) Photoemission and STM Study of the Electronic Structure of Nb-Doped TiO2. Physical Review B, 61 (20), 13445–13457.

[4]   Chen, G. Y., Bare, S. R., and Mallouk, T. E. (2002) Development of Supported Bifunctional Electrocatalysts for Unitized Regenerative Fuel Cells. Journal of The Electrochemical Society, 149 (8), A1092–A1099.

[5]   Fuentes, R. E., García, B. L., and Weidner J. W. (2009) Effect of TiO2 Crystal Structure on the Activity of Pt-Ru towards Electrochemical Oxidation of Methanol. Journal of Electrochemical Society, submitted, March 2010.

[6]   Cassiers, K., Linssen, T., Mathieu, M., Bai, Y. Q., Zhu, H. Y., Cool, P., and Vansant, E. F. (2004) Surfactant-directed synthesis of mesoporous titania with nanocrystalline anatase walls and remarkable thermal stability. The Journal of Physical Chemistry B, 108 (12), 3713–3721.

[7]   Marshall, A., Sunde, S., Tsypkin, M., and Tunold, R. (2007) Performance of a PEM water electrolysis cell using IrxRuyTazO2 electrocatalysts for the oxygen evolution electrode. International Journal of Hydrogen Energy, 32 (13), 2320–2324.